J. Microbiol. Biotechnol. (2016), 26(10), 1668–1674
http://dx.doi.org/10.4014/jmb.1604.04034

jmb

Use of Gold Nanoparticle Fertilizer Enhances the Ginsenoside Contents and Anti-Inflammatory Effects of Red Ginseng

Hee Kang[1], Yun-Gu Hwang[2], Taek-Guen Lee[3], Cheng-Ri Jin[3], Chi Heung Cho[3], Hee-Yeong Jeong[1], and Dae-Ok Kim[3]*

[1]*Graduate School of East-West Medical Science, Kyung Hee University, Yongin 17104, Republic of Korea*
[2]*SMNANOBIO Co., Ltd., Daejeon 34028, Republic of Korea*
[3]*Department of Food Science and Biotechnology, Kyung Hee University, Yongin 17104, Republic of Korea*

Received: April 12, 2016
Revised: July 3, 2016
Accepted: July 7, 2016

First published online
July 19, 2016

**Corresponding author*
Phone: +82-31-201-3796;
Fax: +82-31-204-8116;
E-mail: dokim05@khu.ac.kr

pISSN 1017-7825, eISSN 1738-8872

Red ginseng, a steamed and sun-dried ginseng, is a popular health-promoting food in Korea and other Asian countries. We introduced nanofertilizer technology using gold nanoparticles in an effort to develop red ginseng with an elevated level of ginsenosides, the main active compounds of ginseng. Shoots of 6-year-old ginseng plants were fertilized three times with colloidal gold nanoparticle sprays. Red ginseng extract was prepared from the main roots. The concentrations of gold and ginsenosides were measured following gold nanoparticle treatment. To evaluate the anti-inflammatory effects, mouse peritoneal macrophages of male BALB/c mouse were stimulated with lipopolysaccharide plus interferon-γ in the presence of extracts from red ginseng with or without gold nanoparticle treatment. The content of ginsenosides, such as Rg1, Re, Rf, and Rb1, increased in ginseng treated with gold nanofertilizer whereas the steaming process increased only the levels of Rd and Rg3. The levels of nitric oxide, inducible nitric oxide synthase, and interleukin-6, but not tumor necrosis factor-α, were more suppressed in macrophages treated with extract from gold nanoparticle-treated red ginseng. Our results show that the use of a colloidal gold nanoparticle fertilizer improved the synthesis of ginsenosides in ginseng and enhanced the anti-inflammatory effects of red ginseng. Further research is required to elucidate the causal factors for the gold-induced change in ginsenoside synthesis and to determine the in vivo effect of gold nanoparticle-treated ginseng.

Keywords: Gold nanoparticles, inflammation, macrophages, red ginseng, ginsenoside

Introduction

Korean ginseng, the root of *Panax ginseng* C.A. Meyer, is one of the most popular traditional medicinal plants in East Asia. It is also available as a functional food worldwide. Medicinally, ginseng is used to strengthen body systems weakened by physical and emotional conditions. Many reports have documented the health-enhancing effects of ginseng and its ginsenosides on microbial infections, the immune system, neurodegenerative disease, heart diseases, and cancer treatment [5, 14, 22, 23, 28].

Red ginseng (RG) refers to steamed and sun-dried ginseng, as opposed to white ginseng, which is obtained after a simple drying process. The steaming process of ginseng leads to conversion of various ginsenosides (ginseng saponins), the active components of ginseng [6]. The content of ginsenosides in ginseng root peaks at 6 years after cultivation [22], which makes the 6-year-old-ginseng popular in Korea. With heat treatment, many ginsenosides are converted. Naturally occurring ginsenosides such as Rb1, Rb2, Rc, Rd, Re, Rf, and Rg1 are thermally transformed to F4, Rg2, Rg3, Rg5, Rg6, Rg9, Rg10, Rh1, Rh4, Rk1, Rk3, and Rz1 [17].

Inflammation is a physiological response in a host to eliminate harmful substances by recruiting immune cells from circulation. However, because inflammatory reactions

inevitably damage normal neighboring cells, the duration and intensity of inflammation must be tightly controlled. Among inflammatory cells, macrophages play a critical role in eliminating pathogenic microbes and endogenous damage-associated molecular patterns while attracting white blood cells to the site. Pattern recognition receptors such as Toll-like receptors sense the presence of targets and transmit signals to the nucleus, terminating in rapid expression of cytokines such as tumor necrosis factor (TNF)-α, interleukin (IL)-1, and IL-6, and enzymes that synthesize toxic free radicals and inflammatory lipid mediators [18]. TNF-α, IL-1, and IL-6 cause the vascular inner surface to become sticky, allowing white blood cells to bind to the vessel walls and migrate to injured sites. Inducible nitric oxide synthase (iNOS) produces a toxic compound, nitric oxide (NO), which inflicts nitrosative stress on target molecules [2]. Thus, macrophages have been targeted to control inappropriate inflammatory responses.

There have been attempts to increase the composition of RG by applying various processing methods such as puffing, fermentation, and autoclaving [1, 13, 25]. Recent applications of nanobiotechnology in the area of the agricultural and food sciences have increased the potential to protect plants from phytopathogens and boost food production. Treatment with nanomaterials through nanofertilization technology enhances photosynthetic activity and increases the biomass, fruit yield, and phytomedicine content [10, 16]. Colloidal gold nanoparticles are considered a biocompatible inert metallic form [3]. In this study, a gold nanofertilizer was applied to 6-year-old ginseng, and the ginsenoside composition and anti-inflammatory effects of gold nanoparticle-treated RG and non-treated RG were compared.

Materials and Methods

Preparation of Colloidal Gold Nanoparticles

Colloidal gold nanoparticles were manufactured from SMNANOBIO Co., Ltd (Korea). Preparation of colloidal gold nanoparticles was based on an electrolysis method described by Cheon *et al*. [4]. In brief, two pure gold plates (5 cm × 10 cm × 2 cm) were used as electrodes. The two electrodes were placed vertically face-to-face at a constant distance of 20 mm. Electrolytes consisted of 20 mM sodium citrate, 10 mM citric acid monohydrate, and 0.01% polyvinylpyrrolidone (molecular weight = 29,000 g/mol; Sigma-Aldrich Co., LLC., USA) in deionized water. A pH range of 6.5–7.5, electrolyte temperature of 80–90°C, and current of 20–30 A were applied to obtain the gold nanoparticles. After 30 min, well-dispersed colloidal gold nanoparticles were fabricated in deionized water. The gold nanoparticles were then analyzed by STEM (JEM-2100F; Jeol, Japan) and a zetasizer (ZEN3600; Malvern Instruments Ltd., UK). The size of the gold nanoparticles ranged from 5 to 15 nm [12].

Measurement of Gold in Fresh 6-Year-Old Ginseng Roots

Fourteen days after gold nanoparticle treatment, 60 g of fresh ginseng roots were obtained and dried at 60°C for 10 days. Forty grams of dried ginseng roots was pretreated with nitric acid and analyzed for gold content using an inductively coupled plasma mass spectrometer (Perkin Elmer, USA).

Preparation of Gold Nanoparticle-Treated Red Ginseng

Six-year-old ginseng shoots were treated with gold nanoparticle suspension sprays three times at 14-day intervals. The gold nanoparticle suspension at concentration of 5 mg/l was sprayed in an area of approximately 3.3 m^2 for each treatment. After harvesting, the fresh ginseng roots were sprayed with water to remove foreign matter and steamed at 95°C for 3 h. The steamed ginseng roots were dried first at 60°C for 1 week and then at 40°C for 2 weeks. Five hundred grams of dried roots was soaked in 10 L of distilled water and extracted at 96°C for 24 h. After collecting the supernatant, the roots were again soaked in 8 L of distilled water and re-extracted under the same conditions above. The first and second supernatants were combined and dried at 80°C for 20 h, resulting in the formation of RG solids. After grinding, the powdered RG was dissolved in distilled water for 60°Bx. RG without gold nanoparticle treatment was prepared under the same conditions to those described above. Stock solutions for subsequent cellular assays were filtered using a 0.44 μm filter.

Ginsenoside Analysis

Ginsenosides were analyzed using a high-performance liquid chromatography system (Agilent 1260 series; Agilent Technologies, Inc., Santa Clara, CA, USA) equipped with an auto-sampler, a photodiode array detector, a quaternary pump, and a vacuum degasser. Chromatographic separation was performed using an octadecyl column (Zorbax Eclipse plus C18, 4.6 × 250 mm, 5 μm; Agilent Technologies, Inc.). Gradient flows for the two-solvent system (water as solvent A and acetonitrile as solvent B) were as follows: 80% A/20% B at 0 min, 80% A/20% B at 5 min, 60% A/40% B at 35 min, 60% A/40% B at 45 min, 80% A/20% B at 45.1 min, and 80% A/20% B at 50 min. The flow rate of the mobile phase was 1.0 ml/min with injection volume of 20 μl. Detection was at 203 nm for ginsenosides (Baoji Herbest Bio-Tech Co., Ltd., Baoji, China). The column temperature was set at 30°C.

Isolation of Mouse Peritoneal Macrophages

Seven-week-old male BALB/c mice were obtained from SamTaco (Osan, South Korea) and housed in a temperature- and humidity-controlled pathogen-free animal facility with a 12-h light-dark cycle. The animal protocol (KHUASP(SE)-15-012) was approved by the Kyung Hee University Institutional Animal Care and Use Committee (South Korea) and mice were cared for

according to the US National Research Council for the Care and Use of Laboratory Animals specifications. Mice were intraperitoneally injected with 2 ml of 3.5% sterile thioglycollate solution (BD Sciences, USA), and 4 days later were sacrificed by cervical dislocation. Macrophages were isolated by peritoneal lavage with cold Dulbecco's modified Eagle's medium (DMEM; HyClone, USA). After centrifugation, cells were resuspended in DMEM with 10% fetal bovine serum (FBS; HyClone) and 1% penicillin-streptomycin. Based on flow cytometric analysis, 94% of the peritoneal cells were CD11b-positive macrophages, where CD11b is used as a marker for the identification of macrophages. Peritoneal macrophages were incubated overnight at 37°C with 5% CO_2, and non-adherent cells were removed.

Cell Culture

To measure the effects of RG extract on NO and cytokine levels, peritoneal macrophages were stimulated with 100 ng/ml lipopolysaccharide (LPS) (Sigma-Aldrich Co., LLC.) and 1 ng/ml interferon (IFN)-γ (BD Pharmingen, USA) for 24 h. Supernatant and cells were collected for subsequent assays.

MTS Assay

Peritoneal macrophages were seeded in quadruplicates in 96-well plates and stimulated for 24 h at increasing concentrations of gold nanoparticle-treated RG (herein referred to as gold RG) or non-treated RG. Cell viability was determined using the MTS (3-(4,5-dimethylthiazol-2-yl)-5-(3-carboxymethoxyphenyl)-2-(4-sulfophenyl)-2H-tetrazolium) reduction method (CellTiter96 AQ_{ueous} One Solution Cell Proliferation assay kit; Promega Corp., Madison, WI, USA) based on measurements of mitochondrial respiration in living cells. Absorbance was measured at 490 nm with a microplate reader (iMark; Bio-Rad, USA).

NO Determination

Fifty microliters of supernatant obtained from the culture described above was incubated with an equal volume of Griess reagent (Sigma-Aldrich Co., LLC.) for 15 min at room temperature. Absorbance was measured at 540 nm with a microplate reader (iMark). Sodium nitrite at 0 to 100 μM was used to create a standard curve to calculate the nitrite concentrations.

Cytokine Analysis

The levels of TNF-α and IL-6 in the supernatant were determined by an enzyme-linked immunosorbent assay (ELISA) according to the manufacturer's protocol (BD Pharmingen). In brief, flat-bottomed 96-well plates were coated overnight at 4°C with coating antibodies. The coating antibodies were discarded and the plates were blocked with blocking buffer (10% FBS in phosphate-buffered saline) for 1 h at room temperature. After washing, appropriately diluted samples or standards were added and incubated for 2 h at room temperature. After washing, detecting antibodies plus streptavidin-horseradish peroxidase were added and incubated for 1 h at room temperature. After washing, tetramethylbenzidine substrate solution was added. The color was allowed to develop for 30 min in the dark before the reaction was quenched with 0.2 M H_2SO_4. The plates were then read at 450−570 nm and the sample concentrations were determined from a standard curve.

Western Blotting

Total cell extracts were prepared by resuspending the cells in lysis buffer (50 mM Tris-HCl, pH 7.5; 150 mM NaCl; 1 mM EDTA; 20 mM NaF; 0.5% NP-40; and 1% Triton X-100) containing a phosphatase inhibitor cocktail (Sigma-Aldrich Co., LLC.) and an Xpert protease inhibitor cocktail (GenDEPOT, USA). The protein concentration was determined using the Bradford assay. Cell extracts were separated on 8% or 10% sodium dodecyl sulfate-polyacrylamide gels and were transferred to a polyvinylidene fluoride membrane. The membranes were blocked with 5% skim milk in Tris-buffered saline with 0.1% Tween 20 (TBST) for 1 h and then incubated overnight at 4°C with primary antibody of rabbit polyclonal iNOS or GAPDH (Santa Cruz Biotechnology, USA) diluted 1/1,000 in 5% skim milk in TBST. The blots were washed with TBST and incubated for 1 h with an anti-rabbit horseradish-peroxidase-conjugated secondary antibody (diluted 1:5,000 in 5% skim milk in TBST). Protein bands were detected with EzWestLumi plus (ATTO Corp., Japan) and analyzed using EZ-Capture MG (ATTO Corp.).

Statistical Analysis

Statistical analysis was performed using Student's *t* test or ANOVA followed by the Tukey test using IBM Statistics SPSS ver. 22. The *p*-values of less than 0.05 were considered significant.

Results

Analysis of Gold and Ginsenoside Contents in Ginseng Roots

The content of gold in the main roots of ginseng was measured 14 days after each gold nanoparticle spray was applied to the shoots. The gold content peaked after the first treatment and then decreased with increasing treatment time (Table 1). After the third treatment, the levels of ginsenosides in gold nanoparticle-treated ginseng and non-treated ginseng extracts were comparatively evaluated. In the gold nanoparticle-treated ginseng, the levels of Rg1, Re, Rf, and Rb1 were significantly increased whereas those of Rg2 and Rb3 were significantly decreased compared with non-treated ginseng (Table 2). The sum of ginsenosides was significantly ($p < 0.05$) increased in gold nanoparticle-treated ginseng compared with non-treated ginseng. Steaming at 95°C affected the yield of ginsenosides in both extracts. Among the ginsenosides tested, the levels of Rd, Rg3(*S*), and Rg3(*R*) were significantly increased with gold

Table 1. Contents of gold in the main root of fresh 6-year-old ginseng after colloidal gold nanoparticle treatments[a].

Treatment	Gold content (mg/kg)
1st	0.419
2nd	0.102
3rd	0.040

[a]Gold nanoparticle suspension at concentration of 5 mg/l was sprayed in an area of approximately 3.3 m^2 at a 2-week interval for each treatment.

Table 2. Concentrations of ginsenosides in the main root of fresh 6-year-old ginseng following colloidal gold nanoparticle treatments[a].

Ginsenosides	Concentration (mg/kg)	
	Treated ginseng	Non-treated ginseng
Rg1	14.713 ± 0.473*	11.312 ± 0.198
Rg2	0.154 ± 0.004*	0.179 ± 0.002
Re	2.993 ± 0.005*	1.394 ± 0.017
Rf	0.929 ± 0.004*	0.485 ± 0.024
Rb1	3.442 ± 0.070*	2.553 ± 0.010
Rb3	0.149 ± 0.000*	0.204 ± 0.012
Rd	0.334 ± 0.013	0.207 ± 0.040
Total	22.763 ± 0.454*	16.332 ± 0.243

[a]Data represent the mean ± SD (n = 2). *p < 0.05 versus non-treated group.

nanoparticle treatment, but there was no difference in the sum of ginsenosides (Table 3).

Effect of Gold RG Extract on Cell Viability

First, we determined if the gold RG extract induced cytotoxicity in macrophages. RG extract without gold nanoparticles was used as a control. Peritoneal macrophages isolated from thioglycollate-injected mice were treated with RG or gold RG extracts ranging from 0.0008°Bx to 0.5°Bx for 24 h. Ginseng extract of 1°Bx contained approximately 1.2 g of soluble solids content (data not shown). Cell viability remained unchanged with up to 0.1°Bx of both extracts, but at a higher dose (0.5°Bx), the viability of cells treated with both RG and gold RG extracts decreased (Fig. 1). Subsequently, the following assays were conducted with concentrations no higher than 0.1°Bx.

Effect of Gold RG Extract on LPS/IFN-γ-Induced NO and iNOS

We examined whether there was any difference in the anti-inflammatory effects of RG and gold RG. Macrophages were stimulated with LPS plus IFN-γ for 24 h in the presence of RG or gold RG. Both extracts showed a dose-dependent effect on the reduction of NO (Fig. 2A). At the same concentrations, gold RG showed more potent inhibitory activity than RG. Next, we explored whether the change in NO was due to an altered level of iNOS expression. In cells treated with gold RG, iNOS expression was more inhibited compared with that in cells treated with RG at the same concentrations (Figs. 2B and 2C).

Table 3. Concentrations of ginsenosides in 6-year-old red ginseng with or without gold nanoparticle treatments[a].

Ginsenosides	Concentration (mg/kg)	
	Gold red ginseng	Red ginseng
Rg1	1.916 ± 0.072	2.247 ± 0.103
Re	1.508 ± 0.077	1.394 ± 0.017
Rf	0.403 ± 0.008	0.535 ± 0.030
Rb1	3.744 ± 0.077	4.117 ± 0.265
Rb3	0.154 ± 0.002	0.180 ± 0.015
Rh1	0.756 ± 0.009	0.769 ± 0.069
Rd	0.210 ± 0.014*	0.115 ± 0.012
Rg3(*S*)	0.212 ± 0.004*	0.140 ± 0.013
Rg3(*R*)	0.680 ± 0.016*	0.512 ± 0.043
Total	9.589 ± 0.252	10.237 ± 0.664

[a]Data represent the mean ± SD (n = 2).
*p < 0.05 versus red ginseng.

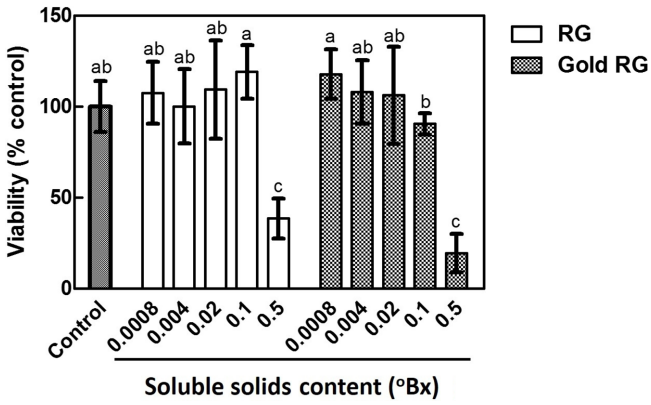

Fig. 1. Effects of red ginseng (RG) and gold RG extracts on the viability of peritoneal macrophages.
Mouse peritoneal macrophages were isolated from thioglycollate-injected male BALB/c mice and cultured with various concentrations of RG or gold RG extracts for 24 h. Cell viability was measured using the MTS assay. Degrees Brix (°Br) expresses the mass percentage of total soluble solids in an aqueous solution. Bars represent the mean ± SD of three independent experiments. Bars with different letters indicate a significant (p < 0.05) difference among groups.

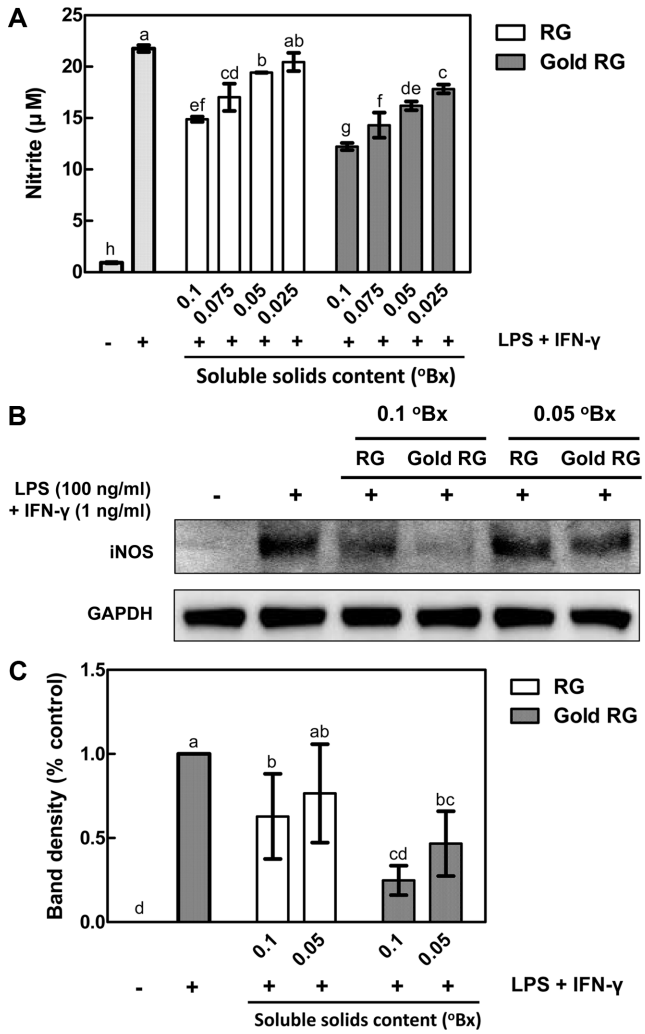

Fig. 2. Effects of red ginseng (RG) and gold RG extracts on nitric oxide (**A**) and inducible nitric oxide synthase (iNOS) expression (**B**), and iNOS band density (**C**) in peritoneal macrophages stimulated with both IFN-γ and LPS.

Cells were stimulated with both LPS (100 ng/ml) and IFN-γ (1 ng/ml) in the presence of extracts from RG or gold RG for 24 h. Levels of nitric oxide in the media were measured by the Griess reaction. The nitrite concentration reflects the amount of nitric oxide generated from the macrophages. Expression of iNOS protein was analyzed by western blotting. One of three independent experiments is shown. GAPDH was loaded as an internal control. Quantification of the immunoblots was carried out by densitometry. Degrees Brix (°Br) expresses the mass percentage of total soluble solids in an aqueous solution. Bars represent the mean ± SD of three independent experiments. Bars with different letters indicate a significant ($p < 0.05$) difference among groups.

Effect of Gold RG Extract on LPS-Induced TNF-α and IL-6 Production

The effects of RG and gold RG extracts on the production of TNF-α and IL-6 in LPS/IFN-γ-stimulated macrophages were compared. Both extracts decreased the levels of TNF-α in a dose-dependent manner, with RG being more potent (Fig. 3A). In contrast, the suppressive effect on IL-6 was more pronounced in cells treated with gold RG (Fig. 3B).

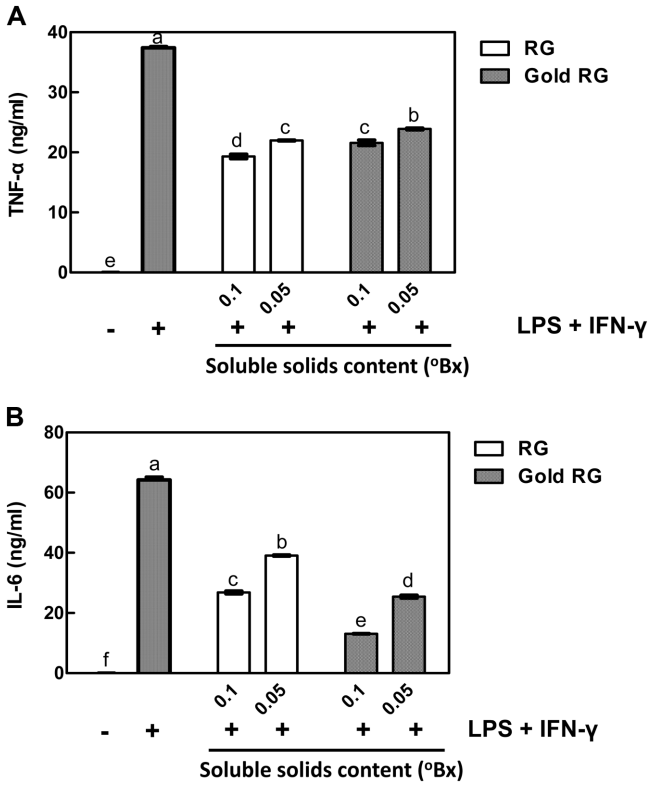

Fig. 3. Effects of red ginseng (RG) and gold RG extracts on tumor necrosis factor (TNF)-α (**A**) and interleukin (IL)-6 (**B**) in peritoneal macrophages stimulated with both IFN-γ and LPS.

Cells were stimulated with LPS (100 ng/ml) plus IFN-γ (1 ng/ml) in the presence of extracts from RG or gold RG for 24 h. The levels of TNF-α and IL-6 in the media were measured by ELISA. Degrees Brix (°Br) expresses the mass percentage of total soluble solids in an aqueous solution. Bars represent the mean ± SD of three independent experiments. Bars with different letters indicate a significant ($p < 0.05$) difference among groups.

Discussion

The application of nanomaterials to food crops has been more recently emerged than the use of nanomaterials in drug delivery and pharmaceuticals. Nanofertilizer technology is expected to improve existing crop management techniques. Nanomaterials of 1–100 nm possess a relatively increased surface area to volume ratio and complexing capability. This property makes nanofertilizers an attractive tool to

promote plant metabolism and growth [9]. Since conventional fertilizers often require repeated application owing to loss of chemicals, degradation by microbes, and photolysis, they can contribute to water and soil pollution. Properly functionalized nanoformulations with high solubility, stability, and effectiveness are expected to reduce such drawbacks [19].

Treatment of the leaf surface of growing ginseng with colloidal gold nanoparticles successfully transferred gold to the main root. Interestingly, gold concentrations in the main root decreased with increasing gold nanofertilizer treatment (Table 1). Gold nanoparticles are assumed to transfer to the lateral and fine roots. For this reason, we speculate that the transfer rate of gold nanoparticles from the main root to the lateral and fine roots was increasing over time. The size of gold nanoparticles employed here ranged from 5 to 10 nm, which is small enough to enter cell wall pores that are 5–20 nm in diameter after penetrating the leaf stromata [20]. Engineered nanoparticles are expected to induce new pores, which will lead to increased internalization of these nanoparticles [20]. From our results, we suspect that new pores might form to facilitate transfer of the gold to the roots.

One of the most significant findings here was that ginsenoside concentrations in the main root of ginseng increased with colloidal gold nanoparticle treatment, indicating that the transfer of gold into the cell had improved ginsenoside synthesis (Table 2). At this point, the causal factors underlying such increases remain to be elucidated. Most studies on the effects of nanoparticles on plant growth and metabolism have been performed at seeding stages [11, 16, 27]. Treatment of bitter melon seed with a carbon-based nanomaterial, fullerol, increased the plant biomass, fruit yield, and phytomedicine content [16]. Spinach seed treated with nano-TiO_2 promoted its photosynthesis and growth [11, 27]. There was also a report that measured the accumulation of airborne iron particles on plant leaf surfaces [8]. Our work is novel because treatment of nanoparticles on the leaf surfaces of mature plants affected the synthesis of secondary metabolites in the root. However, the levels of total ginsenosides were not significantly different between the gold nanoparticle-treated and non-treated RGs (Table 3), indicating that the steaming processing had counteracted the difference. Instead, the yield of Rd and, in particular, Rg3(*S*) and Rg3(*R*), ginsenosides only found in red ginseng, was increased in gold RG. Depending on the preferred type of ginseng or ginsenosides, application of gold nanoparticles may be an alternative tool for ginseng cultivation.

The toxicity of gold nanoparticles has been controversial. In some experiments, gold nanoparticles were toxic both in vitro and in vivo [7, 26]. The gold nanoparticles, which were prepared similarly to those used in this work, proved to be non-toxic up to 13 μg/ml in human intestinal cells and safe after oral administration in rats for 14 days [12]. Exposing cells to gold nanoparticles for a more prolonged period at high concentrations, however, was toxic in cells [12]. Our in vitro cell viability assay showed no significant difference in cell viability between cells treated with RG and gold RG (Fig. 1).

Using an LPS-stimulated macrophage model, we confirmed that the anti-inflammatory effects of gold RG were enhanced compared with those of RG (Figs. 2 and 3). All parameters measured except for TNF-α were more downregulated in cells treated with gold RG. Since production of LPS-induced TNF-α and IL-6 is differentially regulated [15], different components present in RG and gold RG seemed to act in a separate manner. Among the ginsenosides identified in this study, Rg3 and Rd levels increased with gold RG treatment. Rg3 inhibits LPS-induced iNOS, TNF-α, IL-1β, and IL-6 in macrophages [21, 24]. Since ginseng contains acidic polysaccharides and polyphenolic compounds [22], it is possible that components other than ginsenosides are responsible for the increased activity of gold RG.

Taken together, the use of the colloidal gold nanoparticle fertilizer improved ginsenoside synthesis during ginseng cultivation. Moreover, the anti-inflammatory effect of gold RG was enhanced in LPS-stimulated macrophages. Further research is required to validate the causal factors for the gold-induced change in ginsenoside synthesis and the in vivo effect of gold RG.

Acknowledgments

This work was supported by an Inno Polis grant funded by the Korea government (Ministry of Science, ICT and Future Planning) through the Kyung Hee University with grant number A2014DD106.

References

1. Bae HM, Kim SS, Cho CW, Yang DC, Ko SK, Kim KT. 2012. Antioxidant activities of ginseng seeds treated by autoclaving. *J. Ginseng Res.* **36:** 411-417.
2. Bogdan C. 2015. Nitric oxide synthase in innate and adaptive immunity: an update. *Trends Immunol.* **36:** 161-178.
3. Chen H, Dorrigan A, Saad S, Hare DJ, Cortie MB, Valenzuela

SM. 2013. In vivo study of spherical gold nanoparticles: inflammatory effects and distribution in mice. *PLoS One* **8:** e58208.
4. Cheon J, Lee J, Kim J. 2012. Inkjet printing using copper nanoparticles synthesized by electrolysis. *Thin Solid Films* **520:** 2639-2643.
5. Cho IH. 2012. Effects of *Panax ginseng* in neurodegenerative diseases. *J. Ginseng Res.* **36:** 342-353.
6. Christensen LP. 2009. Ginsenosides chemistry, biosynthesis, analysis, and potential health effects. *Adv. Food Nutr. Res.* **55:** 1-99.
7. Chueh PJ, Liang RY, Lee YH, Zeng ZM, Chuang SM. 2014. Differential cytotoxic effects of gold nanoparticles in different mammalian cell lines. *J. Hazard. Mat.* **264:** 303-312.
8. Da Silva LC, Oliva MA, Azevedo AA, De Araújo JM. 2006. Responses of restinga plant species to pollution from an iron pelletization factory. *Water Air Soil Pollut.* **175:** 241-256.
9. de La Rosa G, Lopez-Moreno ML, de Haro-Del Rio D, Botez CE, Peralta-Videa JR, Gardea-Torresdey JL. 2013. Effects of ZnO nanoparticles in alfalfa, tomato, and cucumber at the germination stage: root development and X-ray absorption spectroscopy studies. *Pure Appl. Chem.* **85:** 2161-2174.
10. Gao F, Hong F, Liu C, Zheng L, Su M, Wu X, *et al.* 2006. Mechanism of nano-anatase TiO_2 on promoting photosynthetic carbon reaction of spinach: inducing complex of Rubisco-Rubisco activase. *Biol. Trace Elem. Res.* **111:** 239-253.
11. Hong FH, Zhou J, Liu C, Yang F, Wu C, Zheng L, Yang P. 2005. Effect of nano-TiO_2 on photochemical reaction of chloroplasts of spinach. *Biol. Trace Elem. Res.* **105:** 269-279.
12. Jo MR, Bae SH, Go MR, Kim HJ, Hwang YG, Choi SJ. 2015. Toxicity and biokinetics of colloidal gold nanoparticles. *Nanomaterials* **5:** 835-850.
13. Jung HJ, Choi H, Lim HW, Shin D, Kim H, Kwon B, *et al.* 2012. Enhancement of anti-inflammatory and antinociceptive actions of red ginseng extract by fermentation. *J. Pharm. Pharmacol.* **64:** 756-762.
14. Kang S, Min H. 2012. Ginseng, the 'immunity boost': the effects of *Panax ginseng* on immune system. *J. Ginseng Res.* **36:** 354-368.
15. Kim K, Duramad O, Qin XF, Su B. 2007. MEKK3 is essential for lipopolysaccharide-induced interleukin-6 and granulocyte-macrophage colony-stimulating factor production in macrophages. *Immunology* **120:** 242-250.
16. Kole C, Kole P, Randunu KM, Choudhary P, Podila R, Ke PC, *et al.* 2013. Nanobiotechnology can boost crop production and quality: first evidence from increased plant biomass, fruit yield and phytomedicine content in bitter melon (*Momordica charantia*). *BMC Biotechnol.* **13**: 37.
17. Lee SM, Bae BS, Park HW, Ahn NG, Cho BG, Cho YL, Kwak YS. 2015. Characterization of Korean red ginseng (*Panax ginseng* Meyer): history, preparation method, and chemical composition. *J. Ginseng Res.* **39:** 384-391.
18. Mosser DM, Edwards JP. 2008. Exploring the full spectrum of macrophage activation. *Nat. Rev. Immunol.* **8:** 958-969.
19. Nair R, Varghese SH, Nair BG, Maekawa T, Yoshida Y, Kumar DS. 2010. Nanoparticulate material delivery to plants. *Plant Sci.* **179:** 154-163.
20. Navarro E, Baun A, Behra R, Hartmann NB, Filser J, Miao AJ, *et al.* 2008. Environmental behavior and ecotoxicity of engineered nanoparticles to algae, plants, and fungi. *Ecotoxicology* **17:** 372-386.
21. Shin YM, Jung HJ, Choi WY, Lim CJ. 2013. Antioxidative, anti-inflammatory, and matrix metalloproteinase inhibitory activities of 20(*S*)-ginsenoside Rg3 in cultured mammalian cell lines. *Mol. Biol. Rep.* **40:** 269-279.
22. Wong AS, Che CM, Leung KW. 2015. Recent advances in ginseng as cancer therapeutics: a functional and mechanistic overview. *Nat. Prod. Rep.* **32:** 256-272.
23. Wu H, Hoiby N, Yang L, Givskov M, Song Z. 2014. Effects of radix ginseng on microbial infections: a narrative review. *J. Tradit. Chin. Med.* **34:** 227-233.
24. Yoon SJ, Park JY, Choi S, Lee JB, Jung H, Kim TD, *et al.* 2015. Ginsenoside Rg3 regulates *S*-nitrosylation of the NLRP3 inflammasome via suppression of iNOS. *Biochem. Biophys. Res. Commun.* **463:** 1184-1189.
25. Yoon SR, Lee GD, Park JH, Lee IS, Kwon JH. 2010. Ginsenoside composition and antiproliferative activities of explosively puffed ginseng (*Panax ginseng* C.A. Meyer). *J. Food Sci.* **75:** C378-C382.
26. Zhang XD, Wu HY, Wu D, Wang YY, Chang JH, Zhai ZB, *et al.* 2010. Toxicologic effects of gold nanoparticles in vivo by different administration routes. *Int. J. Nanomed.* **5:** 771-781.
27. Zheng L, Hong FS, Lu SP, Liu C. 2005. Effect of nano-TiO_2 on strength of naturally and growth aged seeds of spinach. *Biol. Trace Elem. Res.* **104:** 83-91.
28. Zheng SD, Wu HJ, Wu DL. 2012. Roles and mechanisms of ginseng in protecting heart. *Chin. J. Integr. Med.* **18:** 548-555.